Letter to the Editor

Synergetic effect by coupling photocatalysis with plasma for low VOCs concentration removal from air

A B S T R A C T

By combining non-thermal plasma and photocatalysis a synergy effect has been observed in low concentrated gaseous isovaleraldehyde oxidation in air. The study of the behavior in isovaleraldehyde oxidation by the separate processes has shown that this synergy effect could be due to the activation by UV on TiO$_2$ of the ozone produced by the non-thermal plasma.

According to the results, plasma–photocatalysis system significantly increases the efficiency of isovaleraldehyde removal and tends to favor the complete mineralization of isovaleraldehyde. It means that plasma–photocatalysis system could be a relevant method for the removal of low concentrated volatile organic compounds from air.

© 2012 Elsevier B.V. All rights reserved.

1. Introduction

Indoor and outdoor air quality (IAQ) has received immense attention in the early 1990s. Emission of various volatile organic compounds (VOCs) was one of the causes of air pollution. Many VOCs can cause headaches, eye, nose and throat irritation and dizziness. Control of VOCs was a major problem due to their general use as solvent in industrial processes, their low concentration in polluted air to be treated and the few number of treatment methods.

In order to develop an effective and low-cost method for VOCs treatment, extensive researches have been performed. Recently, several technologies have been developed to decompose these organic pollutants by oxidation. In particular, photocatalytic process using UV-irradiation has been studied by many researchers and has received great attention in various application fields including environment. The HO radicals, which were generated during the photocatalytic process, are able to oxidize these hazardous VOCs [1–6].

In the most recent years, non-thermal plasma has been reported as an effective method for VOCs oxidation, presenting the very interesting properties to be efficient at ambient temperature under atmospheric pressure for short residence times with low energy consumption [7–10]. The use of a catalyst located within or forward the plasma zone has been reported to improve the efficiency in VOC removal and CO$_2$ formation [11–15]. As firstly observed by Thévenet et al. [16], a synergy effect seems to occur when non-thermal plasma and photocatalysis are coupled in the same reactor. In order to study the reality of this possible synergy for VOC elimination, we have developed a reactor configuration which allows combining these two technologies to treat a larger flow rate containing VOC than usually used at laboratory scale. Coupling non-thermal plasma and photocatalysis in the same reactor could allow adding the high selectivity of photocatalysis in CO$_2$ formation and the high efficiency of VOC removal with low energy consumption

of non-thermal plasma, especially for low VOC concentration. Moreover, the combination of these two technologies in the same reactor allows reducing the total size of this air treatment system.

In this study, the effect of the combination of non-thermal plasma with photocatalyst on the decomposition of VOCs has been investigated experimentally at atmospheric conditions. The individual removal efficiency of photocatalysis (using external UV lamp as a light source) and plasma only was also tested for the comparison. Surface dielectric barrier discharge (DBD) was used for the generation of plasma process. Isovaleraldehyde ((CH$_3$)$_2$CHCH$_2$COH) was chosen as VOC since this compound is the main molecule detected in the exhaust gases from animal quartering centers.

2. Experimental setup

2.1. DBD reactor

In order to study the coupling between non-thermal plasma and photocatalysis, a specific reactor was built. This reactor is made by a Pyrex glass tube (inner diameter = 54 mm, wall thickness = 2 mm) as dielectric barrier, so that the catalyst (TiO$_2$ supported on glass fiber material 100 mm × 170 mm, supplied by Ahlstrom Research and Services) can be simultaneously submitted to a surface non-thermal plasma and a UV radiation from UV lamp (Philips UV lamp: TL 8 W/10 FAM; maximum light intensity output at 364 nm) located coaxially inside the reactor tube and protected by a quartz tube. The outer electrode, connected to the ground, is a 100 mm length copper foil wrapped around the glass tube. According to the reactor geometry we can expect that the irradiance of the catalyst is homogeneous and was measured as 41.1 W/m^2.

The non-thermal plasma was obtained by submitting the electrodes to a sinusoidal high voltage ranging from 0 to 25 kV (peak
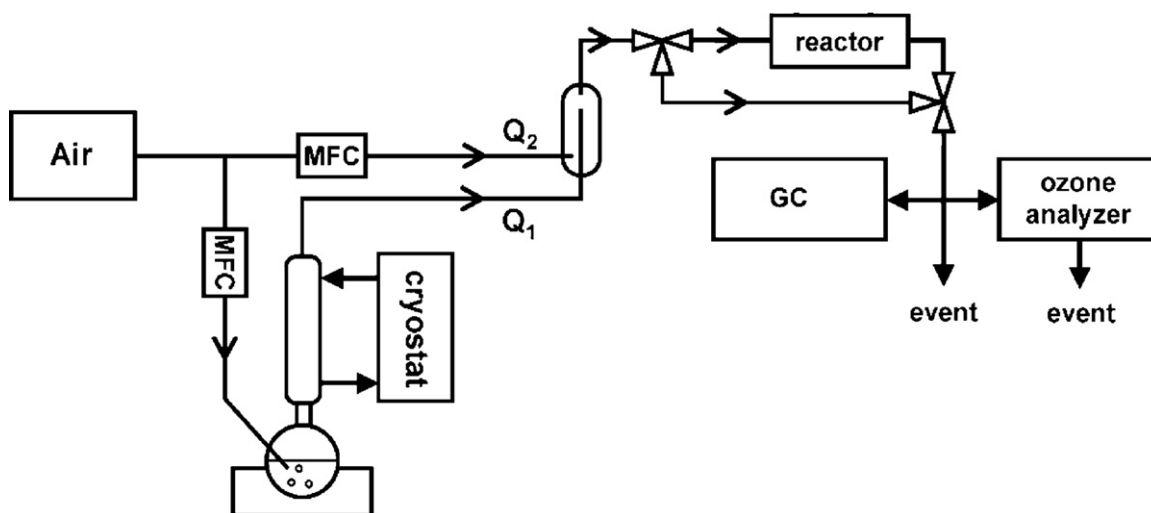
Fig. 1. General scheme of the experimental setup.

to peak) at a 50 Hz frequency. A 500 pF capacitance was positioned between the outer electrode and the ground connection in order to collect the charges transferred through the reactor (Manley's method). Dielectric barrier discharge (DBD) applied voltage (U_a) and high capacitance voltage (U_m) are measured by LeCroy high voltage probes and recorded by a digital oscilloscope (LeCroy LT342, 500 MHz).

The plasma-injected energy by cycle E is calculated by the Lissajous plot method [17] and allows to calculate the power input injected in the reactor as well as the specific energy E_{spe} as follows:

$$P(W) = E(J) \times \text{frequency(Hz)}$$
$$E_{spe}(J/L) = \frac{P(W)}{Q(L/s)}$$

The specific energy value was adjusted by changing the applied voltage (U_a).

2.2. Catalyst preparation

The catalytic material is a fiber glass mat coated with $20 \, g/m^2$ of colloidal silica to ensure the fixation of $20 \, g/m^2$ of PC500 Millenium titanium dioxide nanoparticles. PC500 TiO_2 nanoparticles are 5–10 nm in diameter and are of pure anatase form. The specific area of TiO_2 nanoparticles is $300 \, m^2/g$. The coating process consists in impregnating fibers using industrial size press. Material preparation has been performed by Ahlstrom Research and Services. Preparation process is precisely described into Ahlstrom Patents [18].

2.3. Experimental setup

The experimental setup is shown in Fig. 1. The air–isovaleraldehyde gas mixture (Q_1) was prepared by bubbling synthetic air (Air Liquide) through liquid isovaleraldehyde (Sigma–Aldrich, 97%). The resulting air–isovaleraldehyde gas mixture was passing through a condenser whose temperature is controlled by a cryostat so that the final concentration depends of the vapor pressure of isovaleraldehyde at the condenser temperature. The resulting gas mixture was then diluted by an air flow (Q_2) to obtain the required concentration (30–100 ppmv). The air–isovaleraldehyde or ozone–air–isovaleraldehyde flow was introduced into the reactor at flow rates comprise between

5 and 13 L/min. The Q_1 and Q_2 flow were controlled by mass flow regulators (Brooks 5850 TR). The space velocity through the plasma/photocatalytic zone was in the range between 1895 and $4000 \, h^{-1}$, calculated at ambient temperature and pressure.

2.4. Analyses and procedures

The concentration of isovaleraldehyde before or after the reactor was analyzed by a Varian 430 gas chromatograph equipped with a flame ionization detector (FID) and a CP-Wax58 column (50 m, 0.25 mm). The CO and CO_2 concentrations were analyzed by a two-ways gas chromatograph (μGC Varian Quad CP4900). A Poraplot Q column (10 m, 0.15 mm) and a molecular sieve 5 A (10 m, 0.32 mm) were used with TCD detectors to analyze on-line the concentrations of CO and CO_2 within 3 min. Ozone was monitored on-line by an ozone analyzer (Dual Beam 205 InDevR 2B). All the values are determined at steady state, so that possible adsorption does not contribute to the removal rate. Moreover, the carbon balance was carefully checked to be sure that no carbon deposit occurs.

The isovaleraldehyde (iVA) conversion is expressed as:

$$\text{iVA conversion}(\%) = \frac{c_{in} - c_{out}}{c_{in}} \times 100$$

The formation yields (CO, CO_2 and acetone) are expressed as the percentage of initial isovaleraldehyde concentration converted to the considered product, and the selectivities are calculated as the percentage of disappeared isovaleraldehyde converted to the considered product. The selectivities are normalized to the detected products (CO, CO_2 and acetone), so that the sum of the selectivities was always equal to 100%.

3. Results

Five kinds of experiments have been carried out in order to understand the interaction between non-thermal plasma and photocatalytic material:

- *Photocatalysis alone*: TiO_2 photocatalytic material is placed inside the reactor. The UV lamp is on, no voltage is applied, no discharge is obtained.

- *Plasma alone*: Without catalyst and without UV irradiation. Non-thermal plasma is the only oxidative process performed. The effect of plasma-injected energy on isovaleraldehyde removal has been studied for two different input power 0.88 W and 1.4 W.
- *Plasma and catalyst*: TiO_2 glass fiber coated material is placed inside the reactor but without UV irradiation. Two input power have been studied: 0.88 W and 1.4 W in order to evaluate their influence on isovaleraldehyde removal.
- *Plasma and irradiated catalyst*: TiO_2 glass fiber coated material is placed inside the reactor, the plasma and the UV lamp are on.
- *Photocatalysis in the presence of ozone*: TiO_2 photocatalytic material is placed inside the reactor. Without plasma, the UV lamp is on and ozone is added to the flow rate.

Whatever the technique used (plasma, photocatalysis and combined process), the main reaction products are acetone, carbon dioxide and carbon monoxide, the carbon balance estimated from these three products being always higher than 95% (Table 1).

3.1. Coupling of non-thermal plasma and photocatalysis

Table 1 illustrates the results for isovaleraldehyde conversion and products selectivity for the photocatalysis alone (UV), non-thermal plasma alone (with and without TiO_2 catalyst) and for the coupling of non-thermal plasma and photocatalysis. By photocatalysis alone (irradiation of TiO_2 by UV light at 364 nm), 33% of the isovaleraldehyde was removed, with a CO_2 selectivity of 70%. When non-thermal plasma alone was used, the isovaleraldehyde conversion reaches 39% without catalyst and 44% with TiO_2 catalyst, but the CO_2 selectivity is only comprises between 37 and 41%.

By coupling non-thermal plasma and photocatalysis, the isovaleraldehyde conversion increased to 85% whereas the CO_2 selectivity is about 54%, an intermediate value between photocatalysis alone and plasma alone. Although the isovaleraldehyde conversion by coupling plasma and photocatalysis was 8% higher than the sum of the conversions recorded in the same conditions for plasma alone and photocatalysis alone we cannot unambiguously conclude to the presence of a synergy effect since the concentration of isovaleraldehyde decreases from the entrance to the exit of the reactor modifying then the reaction rates of photocatalysis and non-thermal plasma oxidation. In order to conclude on a possible synergy effect, we have to simulate the reactor behavior by considering only additive effects for each reaction way. The comparison between the simulated values for isovaleraldehyde conversion and the experimental one will allow concluding whether or not a synergy effect occurs by coupling non-thermal plasma and photocatalysis.

3.2. Effect of flow rate

The effect of the residence time on the conversion of isovaleraldehyde and on the CO_2 yield is illustrated in Fig. 2 for the combined processes. The experiments were done at initial concentration of 50 ppmv and 0.88 W of plasma input power. As expected, the conversion increases due to the combined effect of the increase of both the residence time and the energy density.

3.3. Effect of initial concentration of isovaleraldehyde

Another parameter that we analyzed in the degradation of isovaleraldehyde by coupling non-thermal plasma and photocatalysis was the initial concentration of isovaleraldehyde. The flow rate (10 L/min) was constant for all the initial concentrations used for

Table 1
Isovaleraldehyde (50 ppm) conversion, products selectivity, residual ozone concentration at the exit of the reactor and carbon balance for the different tested configurations (room temperature, plasma input energy density = 5.4 J/L).

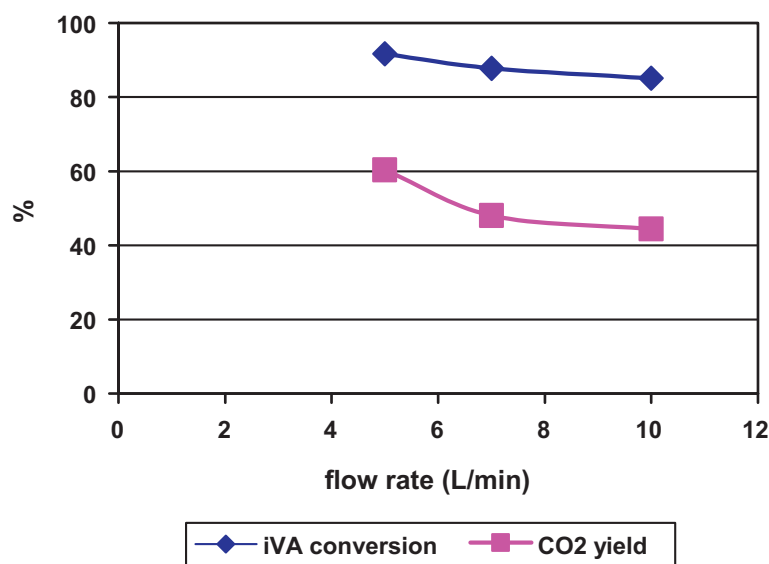|	iVA conversion (%)	Product selectivity (%)			Residual O_3 (ppm)	Carbon balance (%)
		CO_2	CO	$(CH_3)_2CO$		
UV	33.2	70.4	2.2	27.4	0	99.3
Plasma without TiO_2 catalyst	39.2	37.4	9.0	53.6	42	92.5
Plasma with TiO_2 catalyst	44.2	40.8	6.3	52.9	32	94.8
Plasma + UV	85.1	53.9	6.4	39.7	21	96.9

Fig. 2. Effect of flow rate on isovaleraldehyde conversion and CO_2 yield (room temperature, 50 ppmv isovaleraldehyde, plasma-injected power: 0.88 W).

Table 2
Influence of initial concentration on conversion of isovaleraldehyde and on the products selectivity (room temperature, plasma input energy density = 5.4 J/L).

iVA concentration (ppmv)	iVA conversion (%)	Product selectivity (%)		
		CO_2	CO	$(CH_3)_2CO$
30	92.2	55.4	5.4	40.2
50	85.1	53.9	6.4	39.7
70	66.2	33.0	4.8	62.2
100	58.7	28.6	4.7	66.7

this study. The results are shown in Table 2. The isovaleraldehyde conversion decreases with initial concentration of isovaleraldehyde likely due to the well-known behavior of plasma whose efficiency in terms of VOC conversion, for a constant energy density, decreases when the initial concentration increases.

4. Discussion

In order to determine whether or not a synergy effect occurs by coupling plasma and photocatalysis, a simulation of the addition of the two contributions of plasma and photocatalysis can be proposed by assuming that the only interaction between plasma and photocatalysis is due to the separate consumption of isovaleraldehyde by the action of plasma and photocatalysis.

According to previous studies, it is generally admitted that the plasma effect can be modeled by the general expression: $C = C_o \exp(-E_d/\beta)$ where C and C_o are the concentrations of the reactant at the exit and at the entrance of the reactor, respectively, E_d is the energy density (J/L) and β is a parameter which depends on the reactor configuration and on the initial concentration of the reactant. We can expect that the parameter β is of the form $\beta = aC_o$ [19].

Concerning the photocatalysis reaction we can assume that the reaction, for our low concentrations, follows a simple kinetic law with a kinetic order of one relatively to the isovaleraldehyde: $v = -dC/dt = kC$ (with C = isovaleraldehyde concentration). We obtain then: $C = C_o \exp(-k\tau)$ with τ = residence time.

The experimental data allow to roughly determine the different parameters of each process and to simulate the coupling of the

two processes without synergetic interaction by assuming that the reactor can be considered as the addition of successive elementary reactors in order to take into account the decrease of isovaleraldehyde concentration along the reactor.

Calculations have been made by using 10 or 20 elementary reactors without significant change in the results.

For the ith reactor, the isovaleraldehyde exit concentration C_{i+1} is equal to the entrance concentration C_i decreased by the non-thermal plasma and photocatalysis oxidations:

$$C_{i+1} = C_i - \Delta C_{\text{plasma}} - \Delta C_{\text{photocatalysis}}$$

$\Delta C_{\text{plasma}} = C_i - i \exp(-E_d/\beta n) = i(1 - \exp(-E_d/\beta n))$, with n is the total number of elementary reactors and:

$$\Delta C_{\text{photocatalysis}} = C_i - C_i \exp\left(\frac{-k\tau}{n}\right) = C_i \left(1 - \exp\left(\frac{-k\tau}{n}\right)\right)$$

Finally, by combining these expressions and adding $\beta = aC_i$
$C_{i+1} = C_i[-1 + \exp(-E_d/(naC_i)) + \exp(-k\tau/n)]$ where n is the number of elementary reactors, a is a constant ($\beta = aC_i$), k is the rate constant of the photocatalytic reaction and τ is the residence time in the reactor (here, $\tau = 0.9$ s).

For each elementary reactor (ith reactor) we have used the preceding formula to calculate the isovaleraldehyde concentration (C_{i+1}) at the exit of the reactor as a function of the isovaleraldehyde concentration C_i at the entrance of the reactor, the C_{i+1} value being used as the isovaleraldehyde concentration at the entrance of the ($i+1$)th reactor:

Table 3
Comparison between experimental and simulated conversions for the plasma and photocatalysis alone and for combined plasma and photocatalysis for two values of the energy density.

	E_d (J/L)	Plasma alone (%)	Photocatalysis alone (%)	Combined plasma and photocatalysis (%)
Experimental	5.4	44.2	33.2	85.1
Simulated		43.9	33.3	69.8
Experimental	8.4	65.4	33.2	92.9
Simulated		68.9	33.3	89.3

Table 4
Comparison between experimental and simulated conversions for the plasma and photocatalysis alone and for combined plasma and photocatalysis as a function of the initial isovaleraldehyde concentration (energy density = 5.4 J/L).

Initial concentration (ppm)	Combined plasma and photocatalysis (%)		Plasma alone (%)	Photocatalysis alone (%)
	Experimental	Simulated	Simulated	Simulated
30	92.2	90.7	70.9	33.3
50	85.1	69.8	43.9	33.3
70	66.2	59.7	31.7	33.3
100	58.7	52.0	22.3	33.3

The parameters a and k were adjusted from the experimental data obtained with plasma alone e:

$$a = 0.23 \, \text{L/(J ppm)} \quad \text{and} \quad k = 0.45 \, \text{s}^{-1}$$

The results are gathered in Tables 3 and 4.

Whatever the experimental conditions used, experimental results when plasma and photocatalysis are combined show a better efficiency in isovaleraldehyde conversion than the simple addition of the two processes, revealing then an unambiguous synergy effect. The synergy effect appears to be especially important for the plasma energy density of 5.4 J/L where the difference between the additive effect (isovaleraldehyde conversion = 69.8%) and the experimental coupling (isovaleraldehyde conversion = 85.1%). This effect seems to be less important when the total conversion tends toward 100%.

This effect can also be evidenced by varying the initial concentration of isovaleraldehyde, as shown in Table 4.

According to our simulated behavior of only additive effect for non-thermal plasma and photocatalysis we can unambiguously conclude that a synergy effect exists and could participate to an improvement of the efficiency of such kind of VOC elimination technology.

The nature of this effect could be due to several mechanisms occurring when the non-thermal plasma is present since the plasma produces various species such as high energy electrons, excited molecules or radicals (O, N, OH$^\bullet$, O$_2^{\bullet-}$, O$_3$, NO$_2$, NO$_x$, etc.). These molecules can activate the surface of TiO$_2$ material or interact directly with isovaleraldehyde molecules. Roland et al. [20] have suggested that such oxidation improvements are related to the porosity of the structure: porosity would induce a longer residence time of gas species during diffusion through the solid pore system. They also notice a significant role of ozone produced by plasma interacting with material surface. This hypothesis has to be taken into account with TiO$_2$ since a positive effect of ozone on organic compounds photocatalytic oxidation is reported [21].

To explain the observed behavior when non-thermal plasma and photocatalysis are combined several hypothesis can be proposed:

- Activation of TiO$_2$ under high energy electrons generated by plasma can form the same electron–hole pairs that in photocatalysis, increasing then the number of reactive sites.
- Formation of specific active species on the TiO$_2$ catalyst by the action of active species generated by non-thermal plasma [15] on the electron hole pairs formed by UV.
- Plasma electron beam favoring the desorption of intermediary products of oxidation leading to an increase in the turn-over of the catalytic sites.
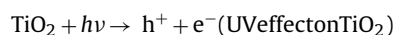
The ozone residual concentration at the exit of the reactor for each configuration (plasma alone, plasma with TiO$_2$ catalyst, photocatalysis alone and the combined process) has been measured (Table 1) and shown a decrease in the range: plasma alone (without catalyst) > plasma with TiO$_2$ catalyst > combined plasma (with TiO$_2$ catalyst) and UV.

These results suggest that UV can play a role either in inhibiting the ozone formation or in ozone elimination.

In order to elucidate the ozone consumption over UV radiations, we have done a series of experiments using O$_3$ as reactant (without isovaleraldehyde in the flow rate). The concentration of ozone (produced by an external device) was maintained at low levels (120 ppmv) in order to reproduce as close as possible the conditions which occur during our experiments. This value corresponds approximately to the ozone concentration obtained by using the plasma alone for $E_d = 17$ J/L ($P = 1.4$ W, air flow rate = 5 L/min). In the absence of TiO$_2$ catalyst, 364 nm wavelength UV radiations were not capable to decompose the ozone molecule. Whereas, in the presence of TiO$_2$ the ozone residual concentration decreases until 89 ppmv, suggesting that in the presence of UV, the TiO$_2$ catalyst becomes active for ozone decomposition.

The consumption of ozone in presence of TiO$_2$ catalyst and under UV irradiation can be explained by two different ways:

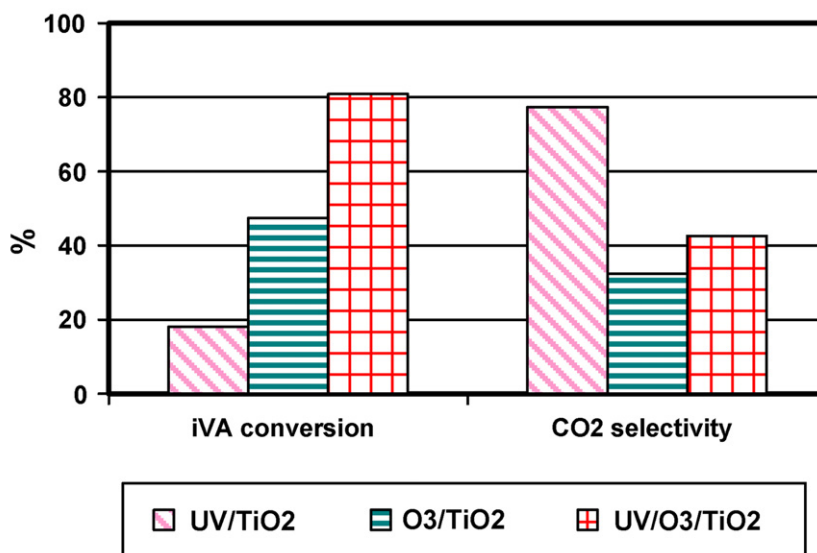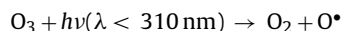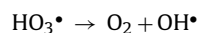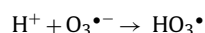- ozone acts as electron acceptor, following this pathway:

$$TiO_2 + h\nu \rightarrow h^+ + e^- (\text{UV effect on TiO}_2)$$

$$O_3 + e^- \rightarrow O_3^{\bullet-} \quad \text{and} \quad O_3^{\bullet-} \rightarrow O^{\bullet-} + O_2$$
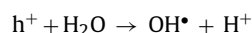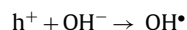
Fig. 3. Isovaleraldehyde conversion and CO_2 selectivity for UV/TiO_2, O_3/TiO_2 and $UV/O_3/TiO_2$ processes (room temperature, 50 ppmv isovaleraldehyde, total flow rate = 13 L/min, 120 ppm O_3 for O_3/TiO_2 and $UV/O_3/TiO_2$ experiments).

• ozone is decomposed by adsorption of photons, as it follows [21]:

$$O_3 + h\nu(\lambda < 310\,\text{nm}) \rightarrow O_2 + O^\bullet$$

According to our results, the mechanism where ozone acts as electron acceptor seems the most likely [22].

The electrons in the conduction band of UV-irradiated TiO_2 are captured either directly or indirectly with the formation of very oxidizing species $O^{\bullet-}$. In addition, the increase in the scavenging rate of photo-produced electrons shown above should decrease the recombination rate of electrons and holes and thereby enhancing the formation rate of hydroxyl radicals from OH surface groups and adsorbed H_2O.

$$h^+ + OH^- \rightarrow OH^\bullet$$

$$h^+ + H_2O \rightarrow OH^\bullet + H^+$$

$$H^+ + O_3^{\bullet-} \rightarrow HO_3^\bullet$$

$$HO_3^\bullet \rightarrow O_2 + OH^\bullet$$

Both species $O^{\bullet-}$ or $OH^\bullet$ are very reactive and can participate to the oxidation of isovaleraldehyde [15].

In order to confirm these hypothesis, 50 ppm of isovaleraldehyde were added to the air/ozone mixture and passed through the reactor at a total flow rate of 13 L/min, without non-thermal plasma but with and without UV irradiation and are compared with the photocatalysis alone, without additional O_3 (Fig. 3).

The results show that the TiO_2 catalyst is slightly active for isovaleraldehyde oxidation by ozone and that the isovaleraldehyde oxidation by ozone is widely improved when the TiO_2 catalyst is irradiated by UV.

The initial ozone concentration is 120 ppm and decreases to 105 ppm at the exit of the reactor when TiO_2 alone is used, whereas this value decreases to 79 ppm when additional UV irradiation is present showing that in the same conditions (UV and TiO_2 catalyst) the presence of isovaleraldehyde increases the ozone consumption. These results show that the UV irradiation is able to both increases the isovaleraldehyde and ozone elimination, suggesting that UVs' are able to activate ozone on the TiO_2 catalyst to improve the isovaleraldehyde oxidation as expected in our proposed mechanism.

This behavior is consistent with the previously proposed mechanism, but the oxidation mechanism by ozone should be slightly different of the photocatalysis mechanism since the CO_2 selectivity appears to be lower for the ozone oxidation than for photocatalysis one.

5. Conclusions

The goal of this paper was to compare the behavior for isovaleraldehyde elimination when photocatalysis and non-thermal plasma are combined, to each process taken separately in order to determine whether or not a synergy effect was present.

We have unambiguously shown that a synergetic effect for the VOC oxidation can be observed when a non-thermal plasma is coupled with a TiO_2 catalyst irradiated by external UV. This effect has been assigned to the possible activation of ozone produced by plasma by the UV radiation in presence of the TiO_2 catalyst.

The behavior of a home-built reactor combining non-thermal plasma and photocatalyst has shown that 50 ppm of isovaleraldehyde can be easily eliminated from an air flow with a low energy consumption allowing proposing this process for industrial use. Moreover, in the particular case of indoor air, the use of an additional catalyst located after the plasma–photocatalysis reactor, able to eliminate the residual ozone should improve the total efficiency of this process.

References

[1] C.H. Ao, S.C. Lee, Applied Catalysis B: Environmental 44 (2003) 191–205.
[2] W.K. Jo, K.H. Park, Chemosphere 57 (2004) 555–565.
[3] M.R. Hoffman, S.T. Martin, W. Choi, D.W. Bahnemann, Chemical Reviews 95 (1995) 69.

[4] A. Dono, C. Paradisi, G. Scorrano, Rapid Communications in Mass Spectrometry 11 (1997) 1687.

[5] B.Y. Lee, S.H. Park, S.C. Lee, M. Kang, C.H. Park, S.J. Choung, Korean Journal of Chemical Engineering 20 (2003) 812.

[6] M.I. Litter, Applied Catalysis B: Environmental 23 (1999) 89.

[7] C. Subrahmanyam, A. Renken, L. Kiwi-Minsker, Chemical Engineering Journal 134 (2007) 78–83.

[8] A.M. Harling, D.A.V.I.D.J. Glover, D.J. Whitehead, J.C.K. Zhang, Environmental Science and Technology 42 (2008) 4546–4550.

[9] J. Van Durme, J. Dewulf, C. Leys, H. Van Langenhove, Applied Catalysis B: Environmental 78 (2008) 324–333.

[10] H.L. Chen, H.M. Lee, Chen, M.B. Chang, S.J. Yu, S.N. Li, Environmental Science and Technology 43 (2009) 2216–2227.

[11] H.-H. Kim, S.-M. Oh, A. Ogata, S. Futamura, Applied Catalysis B: Environmental 56 (2005) 213–220.

[12] S. Futamura, H. Einaga, H. Kabashima, L.Y. Hwan, Catalysis Today 89 (2004) 89–95.

[13] R.B. Sun, Z.G. Xi, F.H. Chao, W. Zhang, H.S. Zhang, D.F. Yang, Atmospheric Environment 41 (2007) 6853–6859.

[14] C. Ayrault, J. Barrault, N. Blin-Simiand, F. Jorand, S. Pasquiers, A. Rousseau, J.M. Tatibouët, Catalysis Today 89 (2004) 75–81.

[15] J. Taranto, D. Frochot, P. Pichat, Industrial and Engineering Chemistry Research 46 (2007) 7611–7614.

[16] F. Thévenet, O. Guaitella, E. Puzenat, J.M. Herrmann, A. Rousseau, C. Guillard, Catalysis Today 122 (2007) 186–194.

[17] T.C. Manley, Proceedings of the 84th General Meeting, New York, 1943.

[18] Ahlstrom Patent EP 1069950; AU 735798 US 09/467, 650; JP 2000-542104.

[19] R. Rudolph, K.P. Francke, H. Miessner, Plasma Chemistry and Plasma Processing 22 (2002) 401–412.

[20] U. Roland, F. Holzer, F.D. Kopinke, Catalysis Today 73 (2002) 315.

[21] B.M. Penetrante, J.M. Bradley, M.C. Hsiao, Japanese Journal of Applied Physics 36 (1997) 5007.

[22] Z. Pengyi, L. Fuyan, Y. Gang, C. Qing, Z. Wanpeng, Journal of Photochemistry and Photobiology A: Chemistry 156 (2003) 189–194.

Alina Maciuca
Catherine Batiot-Dupeyrat
Jean-Michel Tatibouët[*]
*Institut de Chimie des Milieux et Matériaux de
Poitiers (IC2MP), UMR CNRS 7285,
Université de Poitiers,
Ecole Nationale Supérieure d'Ingénieurs de Poitiers,
1 rue Marcel Doré, 86022 Poitiers Cedex, France*

[*] Corresponding author. Tel.: +33 5 49 45 39 02.
E-mail address:
jean-michel.tatibouet@univ-poitiers.fr
(J.-M. Tatibouët)

24 April 2012

Available online 26 June 2012